GBT Memo 308

Errors and Uncertainties in the Project Ranking Scores Generated by the Dynamical Scheduling System

Ronald J. Maddalena, David T. Frayer, Pedro Salas,
Anika Schmiedeke, and Ellie White

October 18, 2022

The algorithms for the Dynamic Scheduling System (DSS), as given in DSS Project Note 5.6 (Condon & Balser, 2015; hereafter DSPN5), require values for performance parameters and weather factors, like night-time pointing errors and wind speeds. Other parameters in the DSS have values that were selected by the authors of DSPN5 out of many possibilities in the hope the chosen values would optimize scientific productivity. Calculated ranking scores, *R*, are then used to rate which observing projects would be the most profitably scheduled. Up to now no memo provides estimates for the accuracy of *R* due to errors or uncertainties in parameters and weather factors. Here we will provide equations for estimating the resulting changes, errors, and uncertainties in *R* from changes, errors, or uncertainties in parameters and weather factors. We then provide a limited number of illustrative, realistic examples on how to use the given equations to explore their effects on *R*. For example, we show how project rankings would change with an improved atmospheric model that corrects for a 30% error in low-frequency zenith optical depths used by the DSS, includes a better model for clouds, and no longer ignores the effects of rain.

I: Introduction

The memos for the Dynamic Scheduling System (DSS) provide no estimate of the errors or uncertainties in calculated ranking scores, *R*. There are a number of advantages if projects had such estimates. For example, projects with similar scores could have very different uncertainties in *R*, which could suggest that the projects with the higher uncertainty have a higher scheduling risk and, thus, may have a higher likelihood of being taken in inappropriate conditions, thereby reducing the scientific productivity of the GBT. If we knew how changes in values of performance parameters altered *R* we could better aim our limited resources at modifying those aspects of telescope performance that would most benefit scheduling and productivity. We could determine how altering the value of open parameters alters scheduling. Error estimates set the accuracy with which we need to know aspects of weather forecasts, like wind speeds or optical depth.

The aim of §II is to provide a set of equations by which one can estimate the uncertainties and errors in *R* due to errors and uncertainties in the various parameters used by the DSS. We assume the reader is familiar with DSPN5, in particular the definitions of the terms in equation 1 of the memo. We will be dealing with the algorithms and values discussed in §3.1, §3.4.1, and 3.4.4 of DSPN5 – atmospheric (η_{atm}), tracking (η_{tr}), and surface (η_{sur}) efficiencies; and observing (l_{eff}) and tracking (l_{tr}) efficiency limits. We will not cover the remaining DSS algorithms for the following reasons:

- The discussions in DSPN5 §3.2 (stringency), 3.3 (pressure factors), and 3.6 (temporal constraints) do net lend themselves to an error analysis.
- Ranking factors (f_x) in DSPN5 §3.5 (e.g., observer on site, thesis project) are single numbers whose values are based on the opinions of the staff. Since *R* is proportional to the product of ranking factors (see equation 1 of DSPN5), then $\Delta R/R = \Delta f_x / f_x$. We assume the reader can calculate these simple ratios.

- Most of the coefficients used in determining performance limits (l_x) in DSPN5 §3.4 are based on the judgment in DSPN5 of what constitutes an unproductive project. Except for l_{eff} the performance limits are Boolean. We also include the effects of the algorithm for l_{tr} as it sets an important frequency-dependent lower limit on η_{tr} below which R is set to zero. Thus, changing parameters in the remaining l_x algorithms will either reduce or increase the number of projects with a non-zero value of R, but they do not change an acceptable project's R.

We will give in §III illustrative examples of how to use the equations of §II. We do not provide a complete survey of the consequences of the equations in §II as there are just too many possible situations. We hope our examples illuminate the relative importance of the factors going into the DSS.

II: Dynamic Scheduling System Equations and Error Estimates

We will use as much as is practical the notation of DSPN5. We will sometimes combine various equations from DSPN5 into one in order to provide a succinct equation that might help the reader understand how the pieces of the DSS are used as a whole. For better understanding we will occasionally separate a DSS equation into equivalent, new equations.

The terms from equation 1 of DSPN5 that we will be dealing with are:

$$R \propto \eta_{atm} \eta_{sur} \eta_{tr} l_{eff} l_{tr} \tag{1}$$

where η are values for the atmospheric, surface, and track efficiencies and l_{eff} and l_{tr} are the efficiency and tracking limits.

II.a: Atmospheric Observing Efficiency, η_{atm}

The algorithms for atmospheric efficiency, η_{atm}, is the square of the ratio of the best possible value for the effective system temperature to the forecasted value for the effective system temperature. Equation 1 combines the various terms and sub-equations that go into η_{atm}. Here we have separated the T_{sys} term in DSPN5 into $T_{sys}=T_\Sigma+T_S$.

$$\eta_{atm} = \left[\left(\frac{T_\Sigma + T_{S<}}{T_\Sigma + T_S} \right) \left(\frac{T_k - T_S}{T_k} \right) \left(\frac{T_{k<}}{T_{k<} - T_{S<}} \right) \right]^2 \tag{2}$$

- T_Σ= the sum of the receiver temperature, elevation-dependent spillover, and the atmospheric-attenuated value of the cosmic microwave background (CMB).
- $T_{S<}$= the atmosphere's contribution to the system temperature under the best conditions for the project's elevation. The total system temperature under the best conditions is $T_\Sigma+T_{S<}$.
- T_S= the atmosphere's contribution to the system temperature for the project's elevation and for the weather conditions that is being scheduled. The total system temperature for the project is $T_\Sigma+T_S$.
- $T_{k<}$= the opacity-weighted mean kinetic temperature of the atmosphere under the best weather.
- T_k= the opacity-weighted mean kinetic temperature for the weather conditions that is being scheduled.

We believe the most intuitive way to present an error analysis is to derive uncertainties or errors in the fractional change in R and η_{atm} since $\Delta R/R=\Delta\eta_{atm}/\eta_{atm}$. For each parameter we provide two versions of an error analysis, one in which the uncertainty or error is small in comparison to the value of the parameter and another that is correct no matter the magnitude of the error or uncertainty. The first version may prove useful for getting a sense of how an error in a parameter affects a project's rating, while the exact version is typically what should be used.

Table 1: Equations for $\Delta R/R$ as a function of errors and uncertainties in parameters for η_{atm} when dealing with T_S.

	Approximate $\Delta R/R$	**Exact $\Delta R/R$**
$\boldsymbol{T_\Sigma}$	$2\left(\frac{1}{T_\Sigma+T_{S<}} - \frac{1}{T_\Sigma+T_S}\right)\Delta T_\Sigma$	$\left[\frac{1+\Delta T_\Sigma/(T_\Sigma+T_{S<})}{1+\Delta T_\Sigma/(T_\Sigma+T_S)}\right]^2 - 1$

	Approximate $\Delta R/R$	Exact $\Delta R/R$
$T_{S<}$	$2\left(\frac{1}{T_\Sigma+T_{S<}}+\frac{1}{T_{k<}-T_{S<}}\right)\Delta T_{S<}$	$\left[\frac{1+\Delta T_{S<}/(T_\Sigma+T_{S<})}{1-\Delta T_{S<}/(T_{k<}+T_{S<})}\right]^2-1$
T_S	$-2\left(\frac{1}{T_\Sigma+T_S}+\frac{1}{T_k-T_S}\right)\Delta T_S$	$\left[\frac{1-\Delta T_S/(T_k-T_S)}{1+\Delta T_S/(T_\Sigma+T_S)}\right]^2-1$
$T_{k<}$	$-2\left(\frac{1}{T_{k<}-T_{S<}}-\frac{1}{T_{k<}}\right)\Delta T_{k<}$	$\left[\frac{1+\Delta T_{k<}/T_{k<}}{1+\Delta T_{k<}/(T_{k<}-T_{S<})}\right]^2-1$
T_k	$2\left(\frac{1}{T_k-T_S}-\frac{1}{T_k}\right)\Delta T_k$	$\left[\frac{1+\Delta T_k/(T_k-T_s)}{1+\Delta T_k/T_k}\right]^2-1$

In some situations working with atmospheric attenuation will fit a problem better:

$$\eta_{atm}=\left[\left(\frac{T_\Sigma+T_{k<}(1-A_<^{-m})}{A^m}\right)\left(\frac{A_<^m}{T_\Sigma+T_k(1-A^{-m})}\right)\right]^2=\left[\frac{(T_\Sigma+T_{k<})A_<^m-T_{k<}}{(T_\Sigma+T_k)A^m-T_k}\right]^2 \tag{3}$$

- m = air mass of the scheduled observation. Approximately equal to sec(z) for zenith distance z.
- $A_<$= zenith attenuation for the best possible weather conditions. $A_<^{-m}=\exp(-m\tau_{Z<})=[1-T_{s<}/T_{k<}]$, where $\tau_{Z<}$ is the zenith optical depth under the best conditions.
- A= zenith attenuation for the weather conditions that is being scheduled. $A^{-m}=\exp(-m\tau_Z)=[1-T_s/T_k]$,where τ_Z is the zenith optical depth under those conditions.

The equations in Table 1 now become:

Table 2: Equations for ΔR /R as a function of errors and uncertainties in parameters for η_{atm} when dealing with zenith atmospheric attenuation

	Approximate $\Delta R/R$	Exact $\Delta R/R$
T_Σ	$2\left(\frac{1}{T_\Sigma+T_{k<}(1-A_<^{-m})}-\frac{1}{T_\Sigma+T_k(1-A^{-m})}\right)\Delta T_\Sigma$	$\left[\frac{1+\Delta T_\Sigma/(T_\Sigma+T_{k<}(1-A_<^{-m}))}{1+\Delta T_\Sigma/(T_\Sigma+T_k(1-A^{-m}))}\right]^2-1$
$A_<$	$2m\left(\frac{(T_\Sigma+T_{k<})A_<^m}{(T_\Sigma+T_{k<})A_<^m-T_{k<}}+1\right)\frac{\Delta A_<}{A_<}$	$\left[\frac{(T_\Sigma+T_{k<})(A_<+\Delta A_<)^m-T_{k<}}{(T_\Sigma+T_{k<})A_<^m-T_{k<}}\right]^2-1$
A	$-2m\left(\frac{(T_\Sigma+T_k)A^m}{(T_\Sigma+T_k)A^m-T_k}\right)\frac{\Delta A}{A}$	$\left[\frac{(T_\Sigma+T_k)(A+\Delta A)^m-T_k}{(T_\Sigma+T_k)A^m-T_k}\right]^{-2}-1$
$T_{k<}$	$2(1-A_<^{-m})/T_\Sigma+T_{k<}(1-A_<^{-m})\Delta T_{k<}$	$\left[1+\Delta T_{k<}(1-A_<^{-m})/(T_\Sigma+T_{k<}(1-A_<^{-m}))\right]^2-1$
T_k	$-2(1-A^{-m})/(T_\Sigma+T_k(1-A^{-m}))\Delta T_k$	$\left[1+\Delta T_k(1-A^{-m})/(T_\Sigma+T_k(1-A^{-m}))\right]^{-2}-1$

II.b: Surface Observing Efficiency

By the definitions in DSPN5 the nighttime (n) surface observing efficiency, $\eta_{sur,n}$, is always equal to one. Equation 9 of DSPN5 gives the daytime (d) values:

$$\eta_{sur,d}=\exp\left[-32\pi^2(\epsilon_d^2-\epsilon_n^2)(v/c)^2\right]. \tag{4}$$

where ν is a project's observing frequency. Only two parameters are involved:

- ε_d = estimated value for the daytime rms of the surface.
- ε_n = estimated value for the best nighttime rms of the surface.

Following the same method as above:

Table 3: ΔR /R as a function of errors and uncertainties in parameters for η_{sur}.

	Approximate $\Delta R/R$	**Exact $\Delta R/R$**
$\boldsymbol{\varepsilon_d}$	$-64\epsilon_d\pi^2(\nu/c)^2\Delta\epsilon_d$	$\exp(-32\pi^2(\nu/c)^2(2\epsilon_d\Delta\epsilon_d+\Delta\epsilon_d^2))-1$
$\boldsymbol{\varepsilon_n}$	$64\epsilon_n\pi^2(\nu/c)^2\Delta\epsilon_n$	$\exp(-32\pi^2(\nu/c)^2(2\epsilon_n\Delta\epsilon_n+\Delta\epsilon_n^2))-1$

II.c: Tracking Observing Efficiency

For tracking efficiency, η_{tr}, we have combined equations 11 through 14 of DSPN5. The algorithms are different for nighttime (n) and daytime (d) observing:

$$\eta_{tr,n}=\left[\frac{(1+F\sigma_{0n}^2)}{(1+F\sigma_{0n}^2+F\cdot(V/a)^4)}\right]^2$$
$$\eta_{tr,d}=\left[\frac{(1+F\sigma_{0d}^2)}{(1+F\sigma_{0d}^2+F\cdot(V/a)^4)}\right]^2 \tag{5}$$

- σ_{0d} and σ_{0n} are the daytime and nighttime tracking plus pointing errors in arcsec under zero wind speeds,
- V = wind speed,
- "a" = the estimated wind speed that will produce a 1 arcsec pointing fluctuation.

For filled-array receivers substitute in equation 5 ε_0, the two-dimensional tracking error, for both σ_{0d} and σ_{0n}. Since the substitution is trivial, and since there are currently no filled-array receiver, we will not present separate equations for filled-array receivers. DSPN5 assumes feeds on all receivers and at all frequencies have a taper, T_e, of 13 dB. Since this is clearly not the case (e.g., Mustang2, L-band, UWBR), we have created F as a way to include the effects of different tapers. Combining the equations for beam width from Maddalena (2010a) with the equations in DSPN5 gives:

$$F=\frac{4\ln(2)\nu^2}{[630+8.3T_e]^2}\ . \tag{6}$$

Thus, there are four parameters to examine for nighttime tracking efficiencies (V, T_e, "a", and σ_{0n}) and five parameters for daytime (V, T_e, "a", σ_{0d}, and σ_{0n}).

Table 4: ΔR /R as a function of errors and uncertainties in parameters for nighttime η_{tr}.

	Approximate $\Delta R/R$	**Exact $\Delta R/R$**
$\boldsymbol{\sigma_{0n}}$	$4\left[\frac{F\sigma_{0n}}{1+F\sigma_{0n}^2}-\frac{F\sigma_{0n}}{1+F\sigma_{0n}^2+F\cdot(V/a)^4}\right]\Delta\sigma_{0n}$	$\left[\frac{1+F(\sigma_{0n}+\Delta\sigma_{0n})^2}{1+F(\sigma_{0n}+\Delta\sigma_{0n})^2+F\cdot(V/a)^4}\right]^2 x\left[\frac{1+F\sigma_{0n}^2+F\cdot(V/a)^4}{1+F\sigma_{0n}^2}\right]^2-1$
$\boldsymbol{a}$	$\left(\frac{8F\cdot(V/a)^4}{1+F\sigma_{0n}^2+F\cdot(V/a)^4}\right)\left(\frac{\Delta a}{a}\right)$	$\left[\frac{1+F\sigma_{0n}^2+F\cdot(V/a)^4}{1+F\sigma_{0n}^2+F\cdot(V/(a+\Delta a))^4}\right]^2-1$

	Approximate $\Delta R/R$	Exact $\Delta R/R$
V	$\left(\frac{-8F\cdot(V/a)^4}{1+F\sigma_{0n}^2+F\cdot(V/a)^4}\right)\left(\frac{\Delta V}{V}\right)$	$\left[\frac{1+F\sigma_{0n}^2+F\cdot(V/a)^4}{1+F\sigma_{0n}^2+F\cdot((V+\Delta V)/a)^4}\right]^2-1$
T_e	$\left[\frac{\sigma_{0n}}{1+F\sigma_{0n}^2}-\frac{\sigma_{0n}}{1+F\sigma_{0n}^2+F\cdot(V/a)^4}\right]\times \left[\frac{-16\ln(2)\cdot 8.3\nu^2}{(630+8.3T_e)^3}\right]\Delta T_e$	$\left[\frac{1+(F+\Delta F)\sigma_{0n}^2}{1+(F+\Delta F)(\sigma_{0n}^2+F\cdot(V/a)^4)}\right]^2\times \left[\frac{1+F\sigma_{0n}^2+F\cdot(V/a)^4}{1+F\sigma_{0n}^2}\right]^2-1$ where $F+\Delta F=\frac{4\ln(2)\nu^2}{[630+8.3(T_e+\Delta T_e)]^2}$

Table 5: $\Delta R/R$ as a function of errors and uncertainties in parameters for daytime η_{tr}.

	Approximate $\Delta R/R$	Exact $\Delta R/R$
σ_{0n}	$\frac{4F\sigma_{0n}}{1+F\sigma_{0n}^2}\Delta\sigma_{0n}$	$\left[\frac{1+F(\sigma_{0n}+\Delta\sigma_{0n})^2}{1+F\sigma_{0n}^2}\right]^2-1$
σ_{0d}	$\frac{-4F\sigma_{0d}}{1+F\sigma_{0d}^2+F\cdot(V/a)^4}\Delta\sigma_{0d}$	$\left[\frac{1+F\sigma_{0d}^2+F\cdot(V/a)^4}{1+F(\sigma_{0d}+\Delta\sigma_{0d})^2+F\cdot(V/a)^4}\right]^2-1$
a	$\left(\frac{8F\cdot(V/a)^4}{1+F\sigma_{0d}^2+F\cdot(V/a)^4}\right)\left(\frac{\Delta a}{a}\right)$	$\left[\frac{1+F\sigma_{0d}^2+F\cdot(V/a)^4}{1+F\sigma_{0d}^2+F\cdot(V/(a+\Delta a))^4}\right]^2-1$
V	$\left(\frac{-8F\cdot(V/a)^4}{1+F\sigma_{0d}^2+F\cdot(V/a)^4}\right)\left(\frac{\Delta V}{V}\right)$	$\left[\frac{1+F\sigma_{0d}^2+F\cdot(V/a)^4}{1+F\sigma_{0d}^2+F\cdot((V+\Delta V)/a)^4}\right]^2-1$
T_e	$\left[\frac{\sigma_{0n}}{1+F\sigma_{0n}^2}-\frac{\sigma_{0d}}{1+F\sigma_{0d}^2+F\cdot(V/a)^4}\right]\times \left[\frac{-16\ln(2)\cdot 8.3\nu^2}{(630+8.3T_e)^3}\right]\Delta T_e$	$\left[\frac{1+(F+\Delta F)\sigma_{0n}^2}{1+(F+\Delta F)(\sigma_{0d}^2+(V/a)^4)}\right]^2 x\left[\frac{1+F\sigma_{0d}^2+F\cdot(V/a)^4}{1+F\sigma_{0n}^2}\right]^2-1$ where $F+\Delta F=\frac{4\ln(2)\nu^2}{[630+8.3(T_e+\Delta T_e)]^2}$

II.d: Observing Efficiency Limit

The intent of the algorithm in §3.4.1 of DSPN5 is to penalize further any project whose product of observing efficiencies ($\eta=\eta_{atm}\,\eta_{sur}\,\eta_{tr}$) is below a frequency-dependent cutoff value:

$$l_{eff}\times\eta=\eta \text{ when } \eta\geq K_1\langle\eta\rangle+K_2$$

$$l_{eff}\times\eta=\eta\exp\left\{\frac{-[K_1\langle\eta\rangle+K_2-\eta]^2}{2\sigma_{eff}^2}\right\} \text{ when } \eta < K_1\langle\eta\rangle+K_2 \tag{7}$$

K_1, K_2, and σ_{eff} are discretionary constants chosen by the authors of DSPN5. Below 50 GHz $\langle\eta\rangle$ was derived by simulations that incorporate as a function of frequency the availability of good weather, receiver performance, scientific demand, etc.. Above 68 GHz $\langle\eta\rangle = 0.5$, a value chosen by the authors of DSPN5. There are five parameters:

Table 6: ΔR/R as a function of errors and uncertainties in parameters for $l_{eff}\times\eta$ when $\eta < K_1\langle\eta\rangle+K_2$.

	Approximate $\Delta R/R$	**Exact $\Delta R/R$**
K_1	$-\langle\eta\rangle\frac{[K_1\langle\eta\rangle+K_2-\eta]}{\sigma_{eff}^2}\Delta K_1$	$\exp\left\{\frac{-2\Delta K_1\langle\eta\rangle[(K_1+\Delta K_1)\langle\eta\rangle+K_2-\eta]}{2\sigma_{eff}^2}\right\}-1$
K_2	$\frac{-[K_1\langle\eta\rangle+K_2-\eta]}{\sigma_{eff}^2}\Delta K_2$	$\exp\left\{\frac{-2\Delta K_2[K_1\langle\eta\rangle+(K_2+\Delta K_2)-\eta]}{2\sigma_{eff}^2}\right\}-1$
σ_{eff}	$\frac{[K_1\langle\eta\rangle+K_2-\eta]^2}{\sigma_{eff}^3}\Delta\sigma_{eff}$	$\exp\left\{\frac{\Delta\sigma_{eff}(2\sigma_{eff}+\Delta\sigma_{eff})}{\sigma_{eff}^2}\frac{[K_1\langle\eta\rangle+K_2-\eta]^2}{2(\sigma_{eff}+\Delta\sigma_{eff})^2}\right\}-1$
$\langle\eta\rangle$	$-K_1\frac{[K_1\langle\eta\rangle+K_2-\eta]}{\sigma_{eff}^2}\Delta\langle\eta\rangle$	$\exp\left\{\frac{-2\Delta\langle\eta\rangle[K_1(\langle\eta\rangle+\Delta\langle\eta\rangle)+K_2-\eta]}{2\sigma_{eff}^2}\right\}-1$
$\eta=\eta_{atm}\eta_{sur}\eta_{tr}$	$\left[\frac{1}{\eta}+\frac{K_1\langle\eta\rangle+K_2-\eta}{\sigma_{eff}^2}\right]\Delta\eta$	$\left(1+\frac{\Delta\eta}{\eta}\right)\cdot\exp\left\{\frac{\Delta\eta[K_1\langle\eta\rangle+K_2-\eta+\Delta\eta/2]}{\sigma_{eff}^2}\right\}-1$

II.e: Combining Error Estimates

The above equations can be used in a few ways:

1. to study the impact of a change the staff makes for a parameter with discretionary values (e.g., K_1, K_2)
2. to study the impact of an anticipated or measured change in a performance parameter (e.g., "a", ε_d, σ_{0d})
3. determine the resulting uncertainty in R by an estimated uncertainty in a quantity like a forecasted wind speed, T_S, receiver temperature, zenith attenuation, etc.

In these cases, apply the equation for the particular parameter in question.

If instead one wants to determine the consequences of changes or uncertainties in multiple parameters, then one needs to be careful in how to combine the values returned by the above equations, especially if the changes in value are large.

- For cases 1 and 2 and for small changes in values, $\Delta R/R$ can be approximated as the sum of the results from the applicable subset of the above equations.
- For case 3, for small uncertainties, and if the uncertainties have a Gaussian-like distribution, $\Delta R/R$ can be approximated as the root sum of squares of the appropriate subset of equations. Care must be taken when combining uncertainties that have non-Gaussian distributions (e.g., wind speeds when winds are low).

Some factors have partially correlated uncertainties or errors (e.g., T_S and $T_{S<}$, T_k and $T_{k<}$, T_S and T_k, ε_d and ε_n, σ_{0d} and σ_{0n}), which will require some understanding of the correlation before combining values returned by the above equations.

III: Illustrative Examples

In this section we will provide examples of how to use the above equations in determining uncertainties and changes in project rankings from uncertainties and changes in input values. We are not trying to show all possible ways in which one can make use of §II, just those we think might be illuminating to the reader.

All examples use the exact equation in Tables 1-6 or Equations 1-7. Unless noted, we use equation 22 and 22a of DSPN5 for $\langle\eta\rangle$ and the following recommended values in DSPN5 and Maddalena & Frayer (2014):

Performance Parameters	ε_d=0.30 mm	ε_n=0.25 mm	σ_{0d}=2.19"	σ_{0n}=1.32"	a =3.50 m/s	ε_0=0.96"
Parameters with Discretionary Values	T_e=13 dB	σ_{eff}=0.02	K_1=1.1	K_2 = -0.12	f_{low}=0.20	f_{high}=0.22

Before proceeding, we need to address how the atmospheric modeling the DSS uses, developed in 2002, is now outdated. The DSS modeling does not include attenuation by rain, has a very simple model for cloud cover, and underestimates by 30% the zenith optical depth at low frequencies. The statistical weather data in the appendix, derived from NAM vertical forecasts (Maddalena 2008) for the year 2019, uses a better atmospheric model that includes the approximate effects of rain, a better model for clouds, and accurate dry-air attenuation. Other than the examples in §III.c and III.h, the improved modeling does not change any aspect of this memo. We will explicitly state when we are using the 2002 or the improved modeling in the examples.

III.a: T_Σ

The DSS uses $T_\Sigma = T_{rcvr} + 5.7$ K where T_{rcvr}, the frequency-dependent receiver noise temperature, is assumed to be known to infinite accuracy. The 5.7 K is the estimate the DSS uses for the sum of the contributions to the system temperature from the 2.7 K CMB and an elevation-independent spillover (3 K). Thus, the accuracy of project rankings suffer from (1) inaccuracies and uncertainties in the DSS-chosen values for receiver noise temperature; (2) the lack of a model in the DSS for elevation-dependent spillover; and (3) the DSS not accounting for the elevation- and weather-dependent absorption of the CMB by the atmosphere.

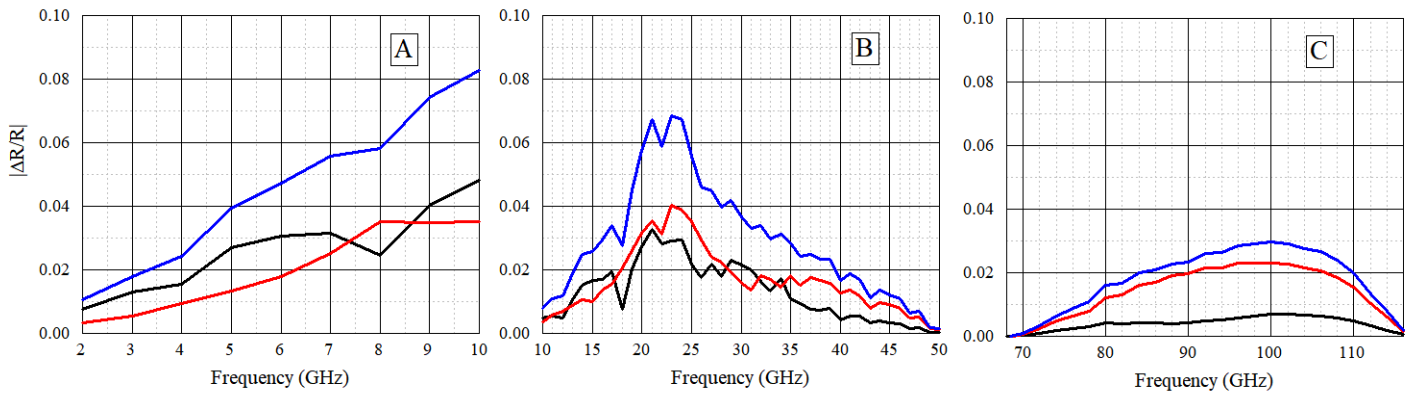

Figure 1: Magnitude of the fractional error or uncertainty in R due to errors or uncertainties in T_Σ. Black is for an offset of 1.5 K, red is for an uncertainty of 10% in receiver noise temperature. Blue is for a combination of a 1.5-K offset and a 10% uncertainty in the case the combination of uncertainties maximizes the magnitude of ΔR/R. Panel A is for 0.90 percentile opacity conditions and m (air mass) = 5; panel B is for 0.25 percentile opacity conditions and m=3; and panel C is for 0.10 percentile opacity conditions and m=3.

We will ignore (3) as it is only relevant when observing at high frequencies and low elevations. From Maddalena & Mattox (2011), spillover is not constant with elevation but varies by ~3 K for all Gregorian receivers, with the highest spillover occurring at high elevations. Receiver noise temperatures probably are known to about 0.5 K at low frequencies but may be uncertain by at least 5 K above 68 GHz. We know that the receiver noise temperatures used by the DSS for Mustang2 are larger than their actual value. As an illustrative example, Figure 1 shows the magnitude of the fractional errors and uncertainties in R for an expected systematic error of 1.5 K (for spillover) and an uncertainty of 10% in receiver noise temperature. The $|\Delta R/R|$ decreases under better weather conditions but does not vary much with elevation.

III.b: $T_{k<}$ and T_k

As we will show in a future memo, forecasted values of T_k *and* $T_{k<}$ the opacity-weighted mean kinetic temperature of the atmosphere, are known to about 2 K (1 sigma). In figure 2 we elected to show fractional uncertainties in R due to a 5 K uncertainties in the forecasted values of $T_{k<}$ and T_k..

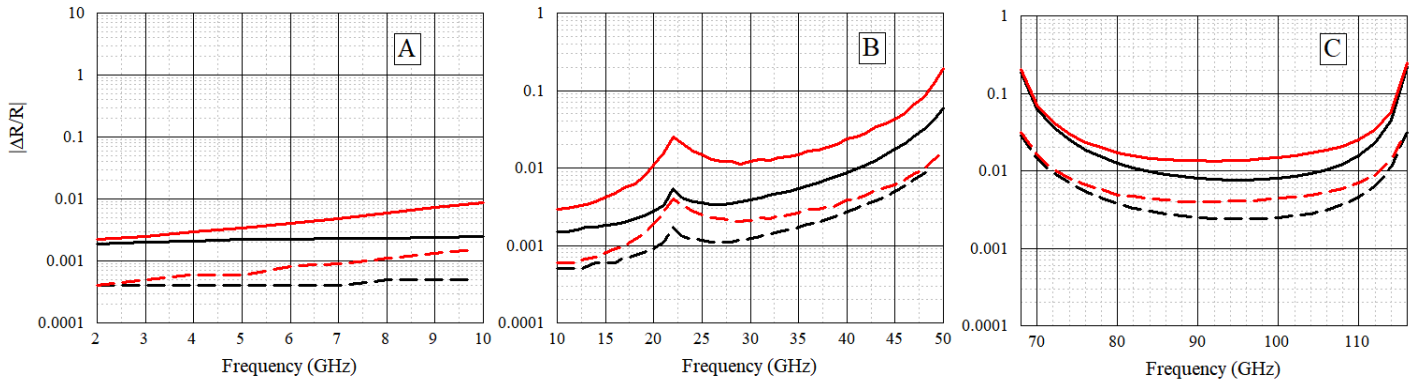

Figure 2: Magnitude of ΔR/R due to 5 K uncertainties in $T_{k<}$ (black) and T_k (red). Panel A is for 0.90 percentile opacity conditions, m = 5 (solid line) and m =1 (dashed line); panel B is for 0.25 percentile opacity conditions, m=3 (solid) and m=1 (dashed); and panel C is for 0.10 percentile opacity conditions, m=3 (solid) and m=1 (dashed).

III.c: $T_{s<}$ and T_s

If the DSS memos specified a desired accuracy for η_{atm}, one can invert the equations in Table 1 to derive the accuracy by which we need to know quantities like T_S. Let us say we wanted an accuracy of $\Delta R/R=\Delta\eta_{atm}/\eta_{atm}<0.10$ at 45 GHz for 0.25 percentile opacity conditions and m=2. Tables 7, 8, and 9 give $\tau_{Z,25\%}$=0.2013, T_k= 266.2 K, and 16.6 K for receiver noise temperature. So, T_Σ=22.3 K (=16.6 K+2.7 K for the CMB+3 K for spillover) and $T_S=T_k[1-\exp(-m\cdot\tau_{z,25\%})]=49.3\,K$). Inverting the equation for ΔT_S in Table 1 gives ~2.6 K as the allowable uncertainty for ΔT_S, or ~5% for $\Delta T_S/T_S$. One would then repeat these steps for all frequencies, weather conditions, and elevations.

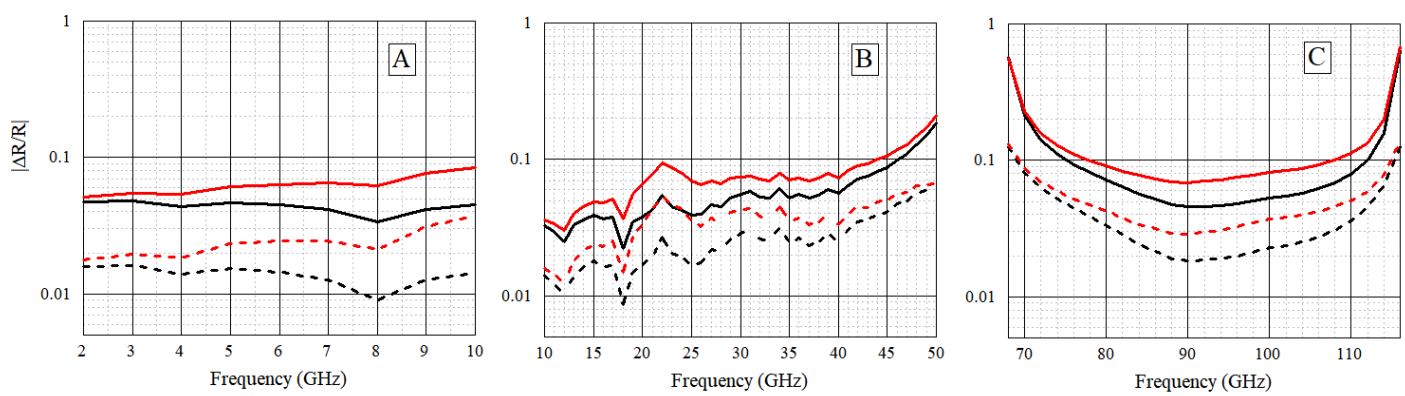

Figure 3: Magnitude of ΔR/R due to a 4% uncertainty in $T_{S<}$ (black) and T_S (red). Panel A is for 0.90 percentile opacity conditions, m = 5 (solid line) and m=1 (dashed line); panel B is for 0.25 percentile opacity conditions, m=3 (solid) and m=1 (dashed); and panel C is for0.10 percentile opacity conditions, m=3 (solid) and m=1 (dashed). At most frequencies a 4% uncertainty is a significant underestimate (see Figure 4) when one considers how the DSS schedules projects.

Figure 3, which uses the equations of Table 1, shows how a 4% fractional uncertainty in ΔT_S and $\Delta T_{S<}$ produces significant uncertainty in R for some observing frequencies. Furthermore, when one considers how the DSS is used to schedule the GBT a 4% fractional uncertainty in T_S is probably an underestimate for most frequencies. Since forecasts are updated every 6 hours, and the GBT is traditionally scheduled up to 48 to 60 hours ahead of time, the T_S used for scheduling will be different than the T_S for when the observations are run. One can use the CLEO forecast software to compare values from the latest forecasts, which can be considered a proxy for the actual conditions at the time of the observations, with those generated when the observations were scheduled. Figure 4 shows for 2019 the fractional change in T_S between forecasts that were 48 hours old and the best available when projects were executed. For better estimates of $\Delta R/R$ that consider how the DSS is used one would combine for more conditions than we could show in Figures 3 and 4 the uncertainty in the current forecasts with the changes in forecasts between when projects are scheduled and executed.

(Observers will be pleased to know that uncertainties in calibration when using forecasted optical depths are typically less than a few percent. For most observations $m \times \tau_Z$ is less than one, and if $\Delta T_S/T_S$ is a few percent for the forecast closest to the time of an observation (i.e., not what is shown in Figure 4 but as demonstrated in Maddalena (2010b)), then the fractional uncertainty in calibration, $m \times \tau_Z \times \Delta T_S/T_S$, will typically be rather low.)

Figure 5 illustrates how to use the equations of §II to understand the consequences of a change in modeling. Panel A shows for a selected sample of observing situations the difference in *exp(-τ)* between the improved and the 2002 models. Panels B and C show respectively η_{atm} for the 2002 models used by the DSS and the improved models. The placement of the η_{atm} curves in panel C, relative to the efficiency-limit curve derived from $\langle\eta\rangle$, suggests that using the new model without updating equation 22 of DSPN5 will severely reduce the hours scheduled for 3-10 GHz observations.

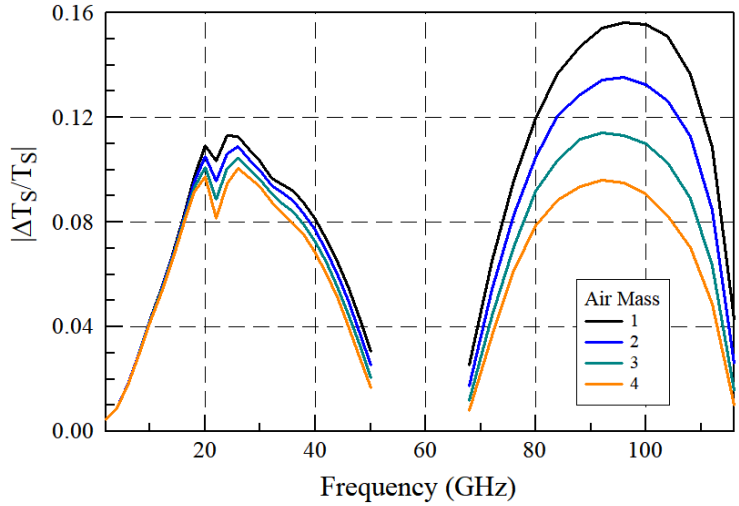

Figure 4: The median of $|\Delta T_s/T_s|$ for the indicated air mass from a comparison of the forecasted T_s when a schedule is generated 48 hours ahead of time with the forecasted T_s at the time of the observation. We derived the curves for only those instances in 2019 with forecasted clear skies.

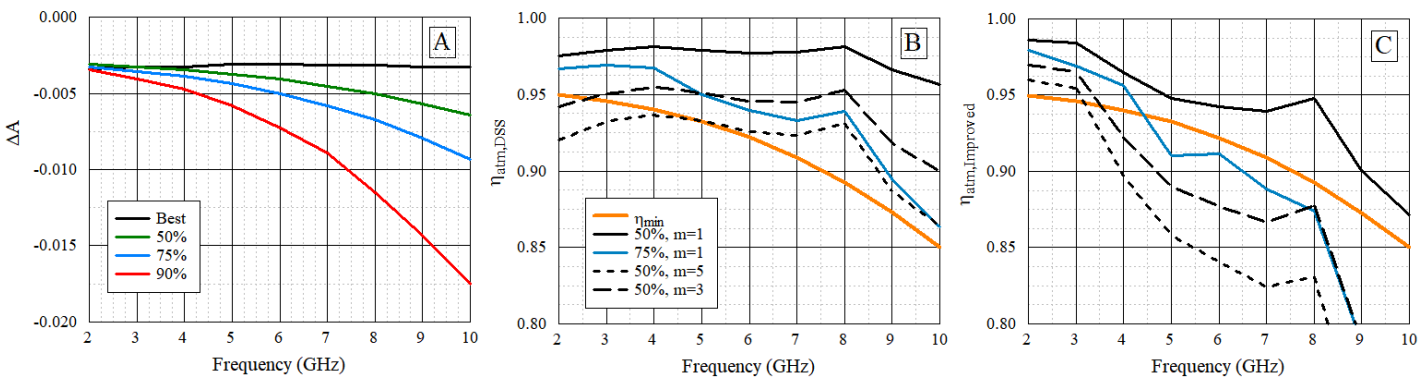

Figure 5: Panel A gives the difference in zenith absorption for different weather conditions between the improved model and the 2002 model used by the DSS. Panel B gives the values of η_{atm} derived from the 2002 model used by the DSS for the indicated weather conditions and air mass, m. Panel C is the same as B except it uses the weather model used by this memo. The orange curve in B and C is, a soft cutoff below which project efficiencies are deemed too poor to be scheduled.

III.d: $\varepsilon_{d<}$ and ε_n

The algorithms used for surface errors in DSPN5 assume that Out-Of-Focus Holography (OOF) is performed as often as is needed during the day and night. In practice most observers do not use OOF during the night below about 40 GHz and do not use OOF during the day below about 30 GHz.

According to DSPN5, all nighttime projects are scheduled using η_{surf} =1 (i.e., the surface is the best possible) at all frequencies. For daytime projects the DSS assumes at all frequencies that the surface has an rms of ε_d, the best that is possible when using OOF during the day. Thus, projects that traditionally select to not use OOF are observing with a poorer surface than what the DSS assumes, and, thus currently are being scheduled with a better value of η_{surf} than they actually deserve. For projects that traditionally elect not to use OOF, the value the DSS should use for the surface rms is that for a completely uncorrected surface, which should be larger than 0.35 mm. In figure 6 we use illustrative rms values of 0.4 and 0.5 mm for the frequency range where observers tend to not follow the assumptions of the DSS.

III.e: *V*

With the adoption of Maddalena & Frayer (2014), the definition for wind used by the DSS is now the same as that used in weather forecasting: 2 minute averages at the top of the hour at a height of 10 m. Forecasted winds rarely get above 8 m/s and are never less than ~0.2 m/s, the latter being a quirk of all weather modeling (Figure 7).

If someone specifies a desired accuracy for η_{tr}, then inverting the equations of Tables 4 and 5 will give the accuracy by which we need to know quantities like wind speed. If we adopt $\Delta R/R=\Delta\eta_{tr}/\eta_{tr}<0.10$ for $V=3.5$ *m/s* at 100 GHz at night, then the ΔV equation from Table 4 gives $\Delta V<1$ m/s. Then, repeat these steps for all frequencies, wind speeds, and feed tapers.

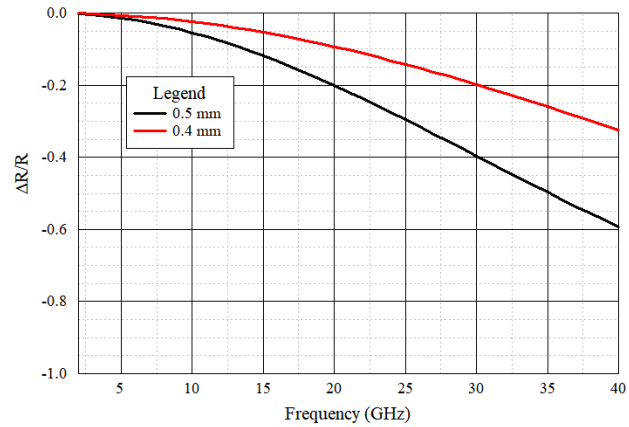

Figure 6: Fractional change in R, assuming the indicated surface rms, when an observer selects not to use OOF. This applies for both daytime and nighttime observations.

An uncertainty of 1 m/s, which we use in the following examples, is also about what we expect considering how the DSS uses forecasted winds. Since forecasts are updated every 6 hours, and the GBT is traditionally scheduled up to 48 to 60 hours ahead of time, one can compare winds from the latest forecasts, which can be considered a proxy for the actual conditions at the time of the observations, with the winds in the forecasts generated many hours previously and which were used for scheduling. The change in winds between forecasts that were 48 hours old and the best available when projects were executed was 0.97 m/s for 2019.

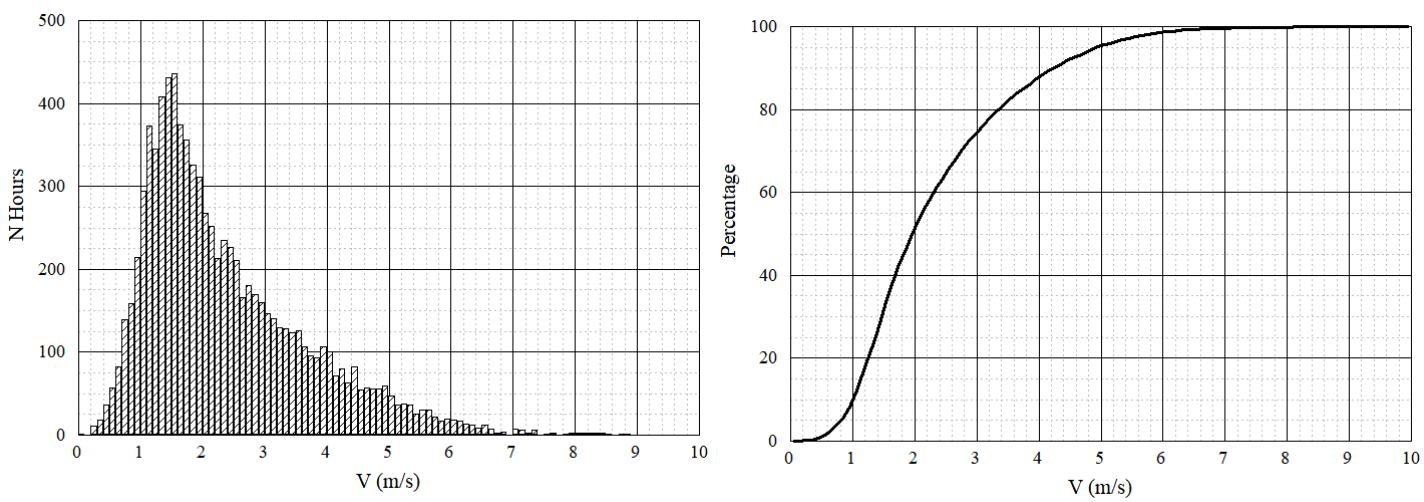

Figure 7: Wind statistics for 2019, presented as a histogram (left) and cumulative distribution (right).

In order to use the equations in Tables 4 and 5, we need to adopt estimates of the wind speeds under which the DSS typically schedules projects. Since projects tend to be scheduled in conditions somewhat below the worse allowable, a reasonable estimate for V might be 0.75 times V_{max}, the limit on winds above which rankings are zero.

When combining DSPN5 §3.1.3 and DSPN5 §3.4 V_{max} exceeds the telescope's wind limit for frequencies below 10 GHz. For higher frequencies V_{max} is given by Equation 8, which combines DSPN5 §3.4.4 and equation 5. We also supply the fractional uncertainties or changes in V_{max} due to uncertainties or changes in various parameters.

$$V_{max}=a\left[\frac{f^2}{\nu^2}(630+8.3T_e)^2-\sigma_0^2\right]^{1/4}$$

$$\Delta V_{max}/V_{max} = \Delta a/a$$

$$\Delta V_{max}/V_{max} = \left[1-\frac{\Delta\sigma_0^2+2\sigma_0\Delta\sigma_0}{f^2(630+8.3T_e)^2/\nu^2-\sigma_0^2}\right]^{1/4}-1$$

$$\Delta V_{max}/V_{max} = \left[1+\frac{(\Delta f^2+2f\Delta f)(630+8.3T_e)^2/\nu^2}{f^2(630+8.3T_e)^2/\nu^2-\sigma_0^2}\right]^{1/4}-1 \qquad (8)$$

$$\Delta V_{max}/V_{max} = \left[1+\frac{8.3f^2\Delta T_e(8.3\Delta T_e+1260+16.6T_e)/\nu^2}{f^2(630+8.3T_e)^2/\nu^2-\sigma_0^2}\right]^{1/4}-1$$

V_{max} depends upon the time of day since σ_0 is either σ_{0n} or σ_{0d}. For single-pixel or non-filled-array receivers, DSPN5 specifies an arbitrary value of f_{low}=0.2 below 50 GHz while Maddalena and Frayer (2014) give weak justification for f_{high}=0.22 for high frequencies. (For filled-array receivers, DSPN5 gives f_{fill}=0.4 and $\sigma_0=\varepsilon_0$, which gives V_{max}=6.5 m/s at 86 GHz, which is 0.99 percentile wind conditions.) Figure 8 shows the current frequency-dependent values for V_{max} as well as how V_{max} changes with values for T_e and f. Readers can explore how a change in "a", σ_{0n}, or σ_{0d} alters V_{max}.

Figure 9 displays $\Delta R/R$ due to a 1 m/s uncertainty in the forecasted wind speed when the wind speed is 0.75 V_{max}. Since an uncertainty of 1 m/s is often a substantial fraction of 0.75 V_{max}, $\Delta R/R$ is not symmetrical around zero.

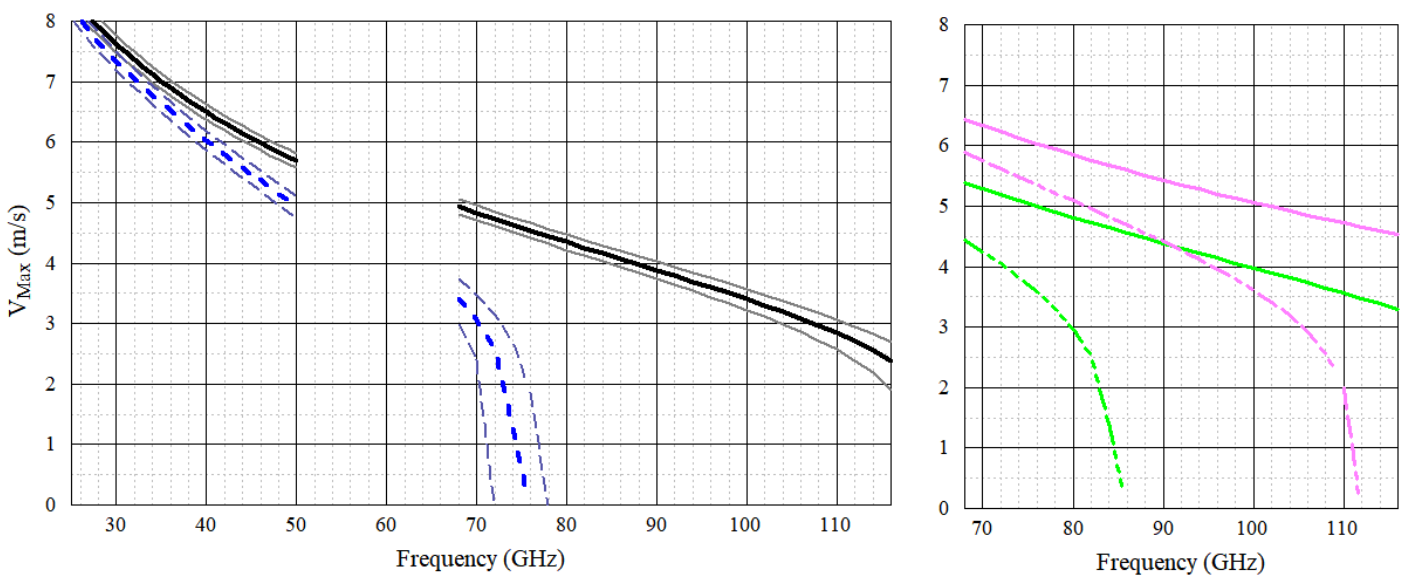

Figure 8: V_{max} for day (solid lines) and night (dashed lines) for non-filled or single-pixel receivers. The left panel uses f_{low} and f_{high} from Maddalena & Frayer (2014); the thick lines are for T_e=13 dB and the thin lines are for 10 and 16 dB (below and above the thick line, respectively). The right panel uses T_e=13 and f_{High}=0.25 (alien green) and 0.33 (alien magenta).

III.f: T_e, "a", σ_{0d} and σ_{0n}

DSPN5 assumes a feed taper of 13 dB, but tapers might differ from this assumption by a few dB. Figure 10 gives the magnitude of the fractional change in R for tapers of 10 and 16 dB. Maddalena & Frayer (2014) state that the formal least-squares fitting error for "a" is 0.05 m/s, but we have doubled that in creating Figure 10.

There are no on-sky measurements of σ_{0d} and σ_{0n} after the major servo upgrade in 2013 from, for example, half-power tracking of astronomical sources. The value for σ_{0n} in Maddalena & Frayer (2014) was inferred from astronomical measurements made years before the upgrade and a rough estimate of how the upgrade might have improved tracking. Maddalena & Frayer's value for σ_{0d} is even less established. In particular, from engineering considerations, it is possible that $\sigma_{0d} = \sigma_{0n}$. For illustration purposes in figure 10 we have used 0.2" as the uncertainty in σ_{0d} and σ_{0n}.

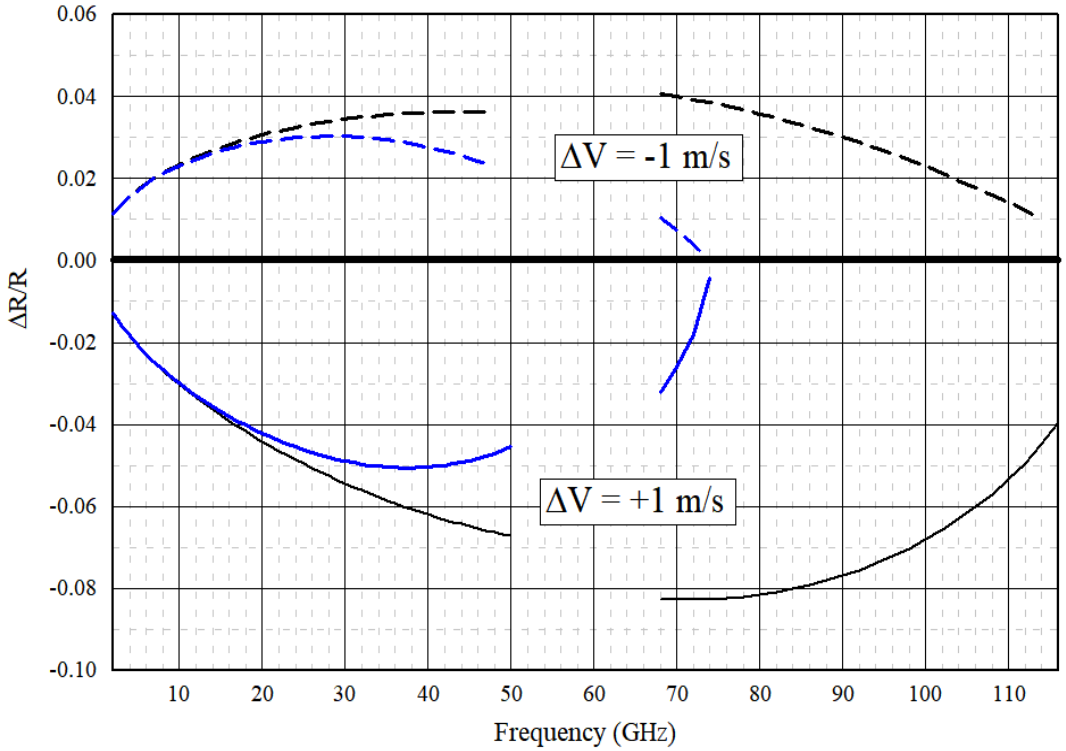

Figure 9: Fractional uncertainty in R for ΔV=±1 m/s and V=0.75 V_{max}. Nighttime projects are in black, daytime in blue. The solid and dashed lines are for ΔV=+1 and -1 m/s, respectively.

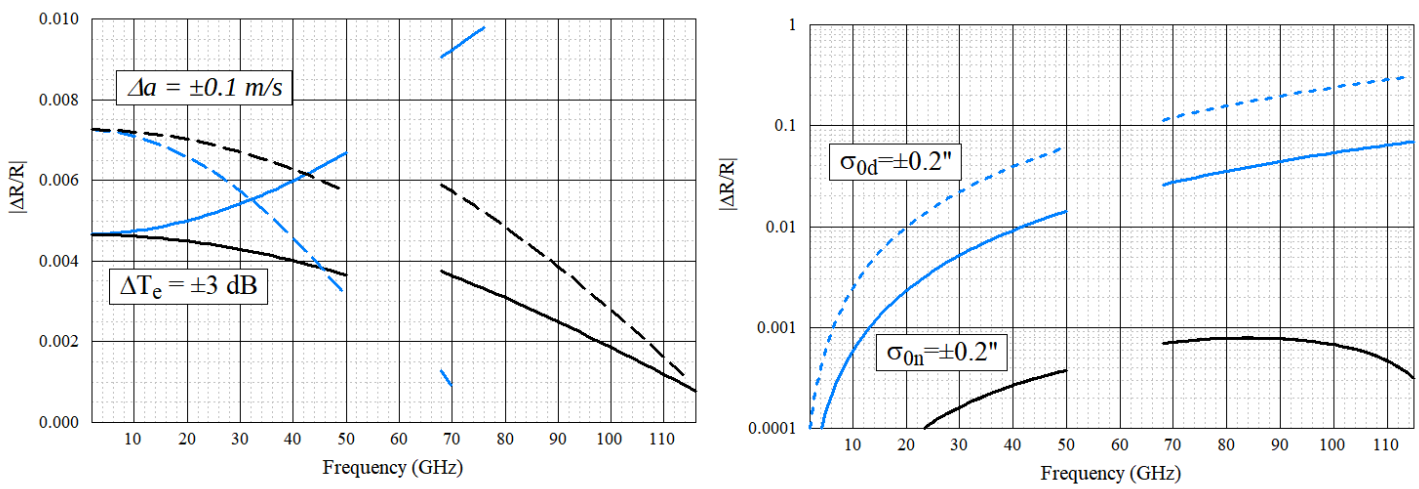

Figure 10: The left panel is the magnitude of the fractional uncertainty in R due to 0.1 m/s uncertainty in "a" (dashed lines) and a systematic error of 3 dB in feed tapers (solid lines). The right panel shows the magnitude of the fractional uncertainty in R due to 0.2 arcsec uncertainties in σ_{0d} (dashed line) and σ_{0n} (solid lines). *The black and blue lines in both panels are the errors or uncertainties for nighttime and daytime, respectively.*

III.g: K_1, K_2, σ_{eff}, η and $\langle\eta\rangle$

The algorithm for l_{eff} is the transformation function given in equation 7 and illustrated as the black line in the sketch at right. In the sketch four projects have the observing efficiencies indicated by the dots. The magenta project would retain its ranking, the red project would not have its ranking downgraded significantly, the green project would have its ranking approximately cut in half, and the project represented by the black dot would have its ranking seriously degraded. The critical point in the transformation equals $K_1\langle\eta\rangle+K_2$ where K_1 and K_2 have arbitrarily-picked values in DSPN5. The DSS uses values for $\langle\eta\rangle$ that were either arbitrary chosen for frequencies above 68 GHz or came from simulations that are now outdated. Small changes in K_1 and K_2 shift the critical point left or right and, thus, could change rankings significantly. Because of the small width of the Gaussian taper, σ_{eff}=0.02, any small changes in a project's observing efficiency, η, can also change project rankings significantly.

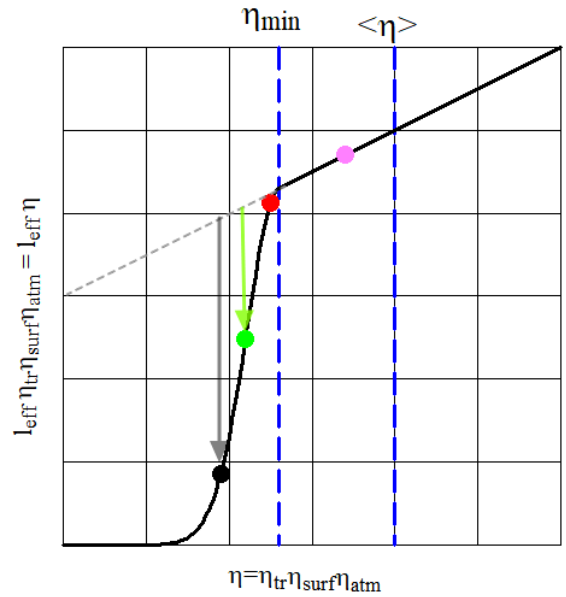

As the analysis in previous subsections suggests, the expected uncertainty and errors in η is rarely smaller than a few percent and is often over 10% in not-too-uncommon situations. In each panel in the following figure, the red dot is illustrative of the value the DSS might derive for η for a project at a frequency above 68 GHz, and the black dots indicate the 1-sigma range in the uncertainty of η due to such factors as an uncertainty in T_s or wind speeds. The project in panel A would have some probability of being scheduled, yet, due to the large uncertainty in η there is some likelihood that doing so would be an ineffective use of the telescope's time. Panel C illustrates a project that the DSS probably would deem unprofitable, yet there is some likelihood that it actually would be a productive use of the telescope's time. The project in panel B falls somewhere in between.

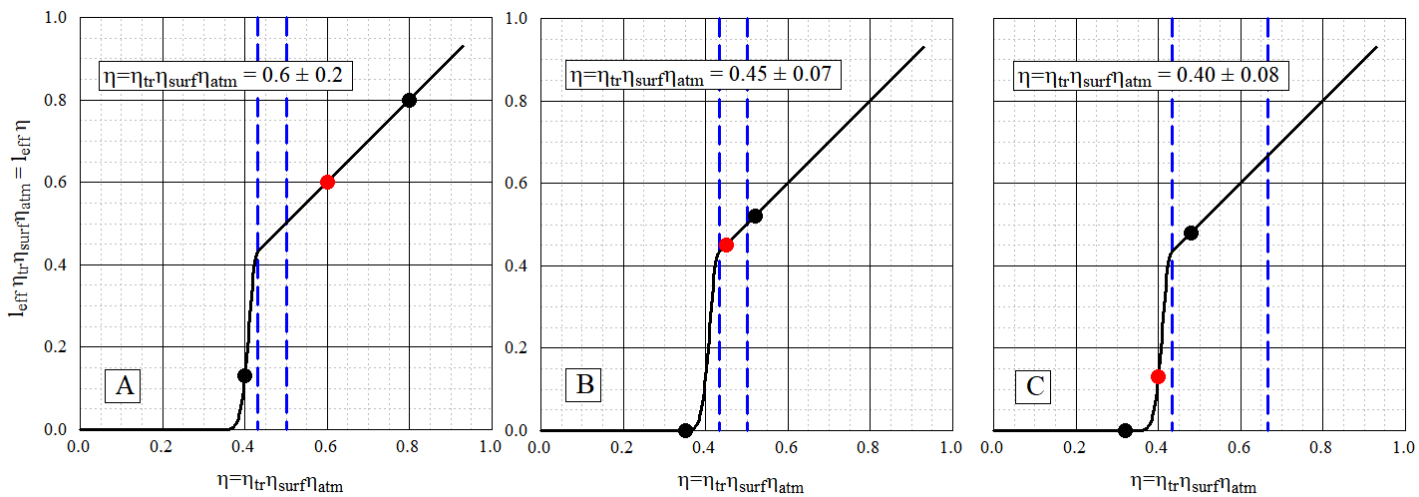

To numerically illustrate the significant consequences to R of small changes to the parameters of equation 7, consider a project at 12 GHz where $\langle\eta\rangle$=0.80. Since $\langle\eta\rangle$ was derived from simulations, it must have some uncertainty which we arbitrarily assign a value of 0.05. The example will use a project that has a reasonable total observing efficiency η=0.74 with an uncertainty of ±0.04, substantially smaller than what §III.a through §III.f implies for 12 GHz. We give the nominal values for K_1, K_2, and σ_{eff} arbitrarily small uncertainties. The following table shows how a small uncertainty in the value of only one parameter in equation 7 produces a large range in possible values for $\eta\times l_{eff}$. The range in output values would be larger if we let two or more parameters simultaneously have uncertainties.

Value and Range in Value	Range in $\eta\ l_{eff}$
K_1=1.1 ± 0.04	0.03 to 0.74
K_2= -0.12 ± 0.02	0.10 to 0.74
σ_{eff}=0.02 ± 0.005	0.30 to 0.54
η=0.74±0.04	0.01 to 0.78
$\langle\eta\rangle$=0.80±0.05	0.004 to 0.74

III.h: A Typical Scheduling Scenario

Frequency	$\tau_{Z<}$	τ_Z	$T_{k<}$ and T_k
22 GHz	0.0213	0.0407	250 K
90 GHz	0.0500	0.0684	253 K
110 GHz	0.0973	0.1231	251 K

For our final example we will consider how uncertainties in two input parameters can schedule the wrong project. Consider three projects that are in competition for the same date and time and differ only in their observing frequencies, 22, 90, and 110 GHz. All are at night for an elevation of 30º and in winds of 3 m/s. We picked a date and time when weather parameters, given in the table to the right, matched those for 10 percentile opacity conditions as determined from the 2002 model used by the DSS. The actual weather conditions give 90 GHz a better ranking than 110 GHz and significantly better ranking than 22 GHz (red lines in Figure 11). In a Monte Carlo simulation of 10,000 trials, we let T_S vary with a 1-sigma deviation of 4% (probably a significant underestimate) and let winds vary with a 1-sigma deviation of 1 m/s. All other parameters had the values given in DPSN5. The simulation calculated three quantities: $\eta=\eta_{atm}\eta_{sur}\eta_{tr}$, $l_{eff}\times\eta$, and $l_{tr}\times l_{eff}\times\eta$. The histograms in Figure 11 depict the range in possible values the DSS would report for R. Note how the DSS will improperly schedule a 22 GHz project over superior 90 and 110 GHz projects about 19% and 55% of the time, respectively. Over 10% of the time the DSS will report 22 GHz rankings substantially below the actual ranking. And, there is about a 25% chance the DSS will improperly pick a 110 GHz project over a higher-ranking 90 GHz project.

Conclusion

The purpose of the memo is to provide a set of tools and examples that use those tools for answering questions about how uncertainties, errors, and changes in values used by the DSS affect a project's R. We hope that the examples are sufficiently varied that one can apply the same methodologies to questions we have not included.

The aim of the memo is certainly not to propose future development of the DSS. Instead, the examples may suggest how to better interpret the output values from the DSS. The following list of suggestions is certainly not complete:

- As Figures 3 and 9 illustrate, the accuracy of η_{atm} and η_{tr} is compromised by small uncertainties in forecasted values for optical depth and winds, often giving uncertainties in η that can exceed 10%. Thus, when multiple projects have η within 10% of each other, the differences in η often will have no statistical significance. Instead of letting η take on a continuum of values, maybe mentally round values of η into five wide bins. Essentially downplay the importance of the relative values of η and increase the significance of the DSS pressure factors P_α^β and P_μ^γ and ranking factors f_{oos}, f_{com}, f_{sg}, and f_{tp}.
- One can consider downplaying the ranking of projects between 20 and 40 GHz as they are getting inappropriately high rankings since standard observing tactics do not follow the DSS assumption about the use of OOF (Figure 6).
- Daytime observing at high frequencies is very sensitive to small changes to the values of f_{high} and σ_{0d} (Figure 8), both of which have values that do not have strong justification. We should consider ways to determine whether the current value for f_{high} is appropriate and to schedule ways to test the value of σ_{0d}.

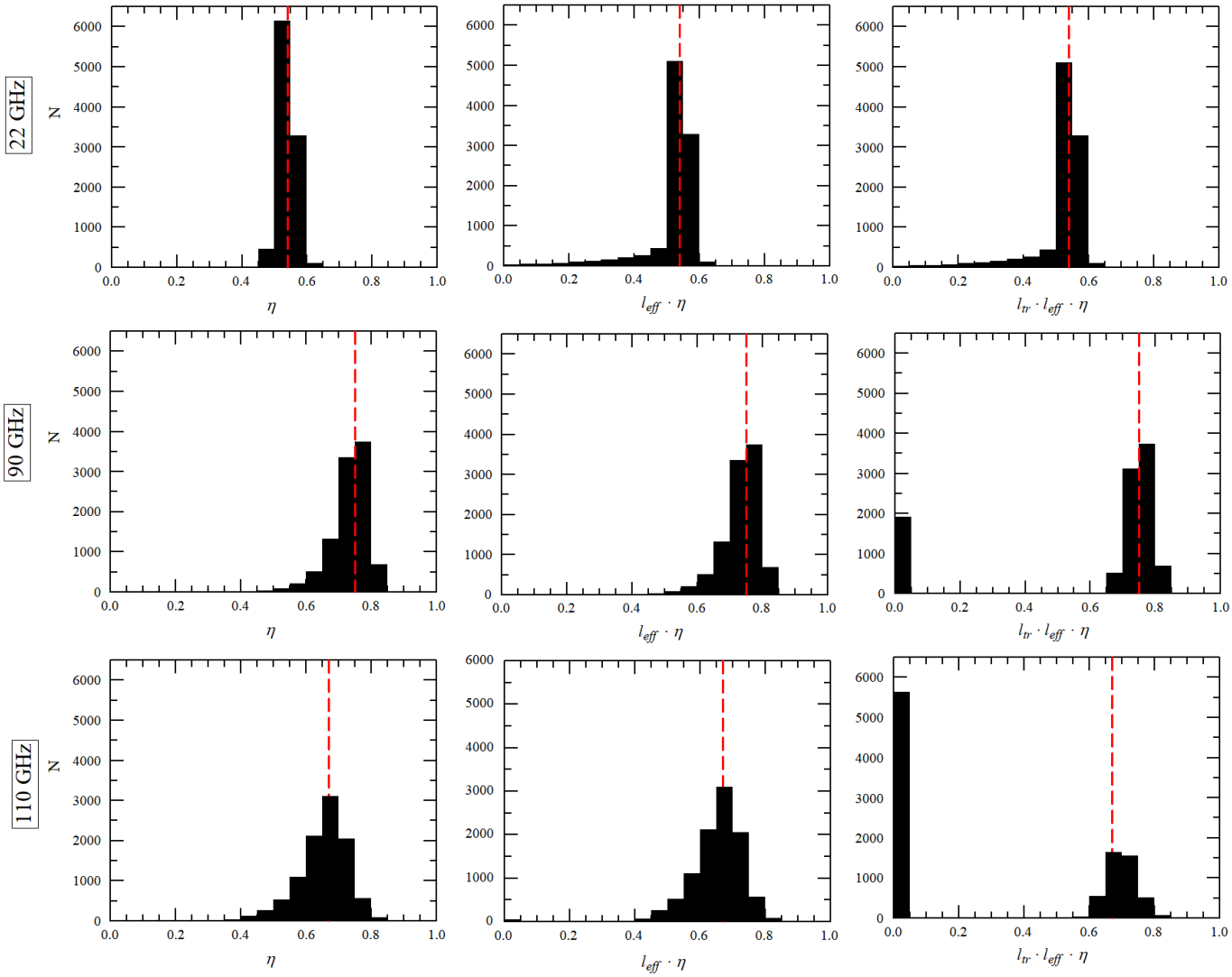

Figure 11: Results of Monte Carlo simulations at 22, 90, and 110 GHz for the typical observing conditions described in the text when applying the 2002 weather model used by the DSS. The vertical lines indicate the actual values for the given weather conditions and the histograms show the range of values the DSS would report when there is a 1 m/s (1-sigma) uncertainty in winds and a 4% (1-sigma) uncertainty in T_S. The right two columns show how the algorithms for efficiency and tracking limits alter observing efficiency and, thus, project rankings.

- Due to the large uncertainties in η_{tr} at high frequencies, the l_{tr} algorithm will often set R to zero when the project has a respectable value for η (e.g., Figure 11). We might consider ways in which to circumvent the l_{tr} algorithm (e.g., setting the discretionary value of f to a large value), a recommendation staff have made over the years.
- When η for a project has a value above $\langle\eta\rangle$ but uncertainties in forecasts place the DSS-calculated value for η just below $\langle\eta\rangle$, the project might not get scheduled due to the sensitivity of R from the discretionary values in the l_{eff} algorithm. As with the l_{tr} algorithm we might consider staff recommendation to circumvent completely the l_{eff} algorithm (e.g., setting the discretionary value of K_1 and K_2 to zero). Circumventing the l_{eff} algorithm would also mean there is then no reason to use resources running simulations to revise $\langle\eta\rangle$.
- η_{atm} has significant systematic errors from using an outdated weather model that mostly affects low-frequency projects. One might consider that all projects at low frequencies have values for R that are inappropriately high (Figure 5) and instead pick a high-frequency project with a respectable R.
- Converting the DSS to the improved weather model would require revising the equation for $\langle\eta\rangle$, but only if the l_{eff} algorithm is retained. This and some of the our other suggestions will require calculating new values for stringencies whose values we believe will then be more reasonable than what are currently being applied.

References

Condon, J. J. & Balser, D. S. 2015, “Dynamic Scheduling Algorithms, Metrics, and Simulations,” Dynamic Scheduling Project Note 5.6

Maddalena, R. J. 2008, “Weather Forecasting For Radio Astronomy: Part I The Mechanisms and Physics”, NRAO Technical Seminar (https://www.gb.nrao.edu/~rmaddale/Research/WeatherForecastingForRadioAstronomy.pdf).

Maddalena, R. J. 2009, “Accurate Weather Forecasting for Radio Astronomy,”, NRAO Technical Seminar (https://www.gb.nrao.edu/~rmaddale/Research/AccurateWeatherForecastingOct2009.pdf).

Maddalena, R. J. 2010a, “Theoretical Ratio of Beam Efficiency to Aperture Efficiency,” GBT Memo 276

Maddalena, R. J. 2010b, “Accurate Weather Forecasting for Radio Astronomy,” Bulletin of the American Astronomical Society, Vol. 42, p.406 (https://www.gb.nrao.edu/~rmaddale/Research/WeatherPosterAASJan2010Mod.pdf).

Maddalena, R. J. & Frayer, D. 2014, “Recommended Changes to the Constants Used by the DSS for Fall 2014,” DS Project Note 18.1

Maddalena, R. J. & Mattox, M. E. 2012 “Accurately Measuring the Spillover of a Radio Telescope,” Bulletin of the American Astronomical Society, Vol. 219 (https://www.gb.nrao.edu/~rmaddale/Research/SpilloverAASJan2012d.pdf)

Appendix

Table 7: Zenith optical depth from 2019 NAM forecasts (Maddalena 2008). A=exp(-τ) and $T_S = T_k\left(1 - A^{-m}\right)$. ***Best*** *and* ***Worse*** *columns are the lowest and highest* τ_Z*, the other columns are 0.10 percentile, 1st, 2nd, 3rd quartile and 0.90 percentile opacities.*

Frequency (GHz)				***Percentile***			
	Best	***0.10***	***0.25***	***0.50***	***0.75***	***0.90***	***Worse***
2	0.0099	0.0102	0.0104	0.0108	0.0112	0.0116	0.0222
3	0.0104	0.0107	0.0109	0.0113	0.0118	0.0131	0.0364
4	0.0107	0.0111	0.0113	0.0117	0.0125	0.0151	0.0567
5	0.0109	0.0114	0.0117	0.0122	0.0135	0.0178	0.0828
6	0.0112	0.0118	0.0122	0.0128	0.0148	0.0211	0.1146
7	0.0114	0.0122	0.0126	0.0136	0.0164	0.0251	0.1523
8	0.0117	0.0126	0.0132	0.0145	0.0184	0.0304	0.1960
9	0.0120	0.0130	0.0138	0.0156	0.0207	0.0362	0.2455
10	0.0124	0.0135	0.0146	0.0170	0.0234	0.0430	0.3010
11	0.0129	0.0140	0.0154	0.0186	0.0265	0.0508	0.3623
12	0.0133	0.0147	0.0165	0.0205	0.0301	0.0598	0.4291
13	0.0138	0.0154	0.0179	0.0228	0.0343	0.0700	0.5015
14	0.0143	0.0163	0.0194	0.0255	0.0392	0.0810	0.5802
15	0.0149	0.0176	0.0212	0.0290	0.0451	0.0931	0.6663
16	0.0156	0.0191	0.0237	0.0337	0.0522	0.1071	0.7554
17	0.0166	0.0211	0.0271	0.0400	0.0617	0.1241	0.8507
18	0.0179	0.0240	0.0318	0.0493	0.0754	0.1462	0.9587
19	0.0197	0.0284	0.0392	0.0643	0.0976	0.1757	1.0821
20	0.0219	0.0355	0.0507	0.0888	0.1341	0.2216	1.2320
21	0.0255	0.0471	0.0692	0.1265	0.1943	0.2902	1.4242
22	0.0396	0.0714	0.1023	0.1833	0.2772	0.3892	1.6639
23	0.0315	0.0611	0.0917	0.1685	0.2606	0.3792	1.7350
24	0.0282	0.0519	0.0767	0.1408	0.2158	0.3402	1.7597
25	0.0276	0.0455	0.0664	0.1168	0.1794	0.3124	1.8091
26	0.0278	0.0420	0.0600	0.1011	0.1588	0.3027	1.8859
27	0.0280	0.0402	0.0565	0.0922	0.1493	0.3037	1.9805
28	0.0288	0.0396	0.0550	0.0880	0.1458	0.3117	2.0867
29	0.0298	0.0399	0.0547	0.0859	0.1463	0.3223	2.2009
30	0.0313	0.0408	0.0553	0.0857	0.1498	0.3365	2.3207
31	0.0330	0.0422	0.0570	0.0870	0.1546	0.3538	2.4441
32	0.0350	0.0440	0.0590	0.0893	0.1609	0.3716	2.5705
33	0.0373	0.0463	0.0616	0.0924	0.1677	0.3913	2.7001
34	0.0400	0.0489	0.0645	0.0962	0.1754	0.4116	2.8319

Frequency (GHz)	Percentile						
	Best	***0.10***	***0.25***	***0.50***	***0.75***	***0.90***	***Worse***
35	0.0430	0.0520	0.0681	0.1007	0.1840	0.4332	2.9662
36	0.0464	0.0556	0.0722	0.1060	0.1937	0.4562	
37	0.0503	0.0598	0.0770	0.1117	0.2040	0.4797	
38	0.0549	0.0645	0.0823	0.1184	0.2152	0.5047	
39	0.0602	0.0701	0.0885	0.1259	0.2275	0.5314	
40	0.0662	0.0767	0.0954	0.1343	0.2409	0.5595	
41	0.0735	0.0843	0.1035	0.1442	0.2557	0.5886	
42	0.0821	0.0933	0.1131	0.1553	0.2718	0.6190	
43	0.0923	0.1040	0.1243	0.1682	0.2898	0.6516	
44	0.1049	0.1171	0.1378	0.1833	0.3099	0.6860	
45	0.1204	0.1332	0.1543	0.2015	0.3331	0.7240	
46	0.1398	0.1534	0.1749	0.2233	0.3605	0.7661	
47	0.1650	0.1794	0.2010	0.2510	0.3932	0.8142	
48	0.1974	0.2136	0.2353	0.2866	0.4339	0.8701	
49	0.2419	0.2607	0.2822	0.3348	0.4876	0.9398	
50	0.3083	0.3305	0.3514	0.4048	0.5628	1.0303	
68	0.5628	0.6064	0.6407	0.7338	0.9929	1.7350	
70	0.3172	0.3496	0.3910	0.4915	0.7623	1.5311	
72	0.2175	0.2478	0.2948	0.4033	0.6836	1.4802	
74	0.1628	0.1930	0.2445	0.3598	0.6512	1.4723	
76	0.1292	0.1604	0.2152	0.3379	0.6394	1.4841	
78	0.1073	0.1397	0.1974	0.3268	0.6402	1.5114	
80	0.0923	0.1259	0.1869	0.3224	0.6461	1.5465	
82	0.0816	0.1166	0.1804	0.3225	0.6574	1.5828	
84	0.0741	0.1106	0.1771	0.3268	0.6714	1.6215	
86	0.0686	0.1068	0.1755	0.3318	0.6870	1.6628	
88	0.0646	0.1044	0.1758	0.3383	0.7050	1.7054	
90	0.0620	0.1033	0.1775	0.3470	0.7234	1.7510	
92	0.0603	0.1033	0.1807	0.3567	0.7436	1.7940	
94	0.0594	0.1043	0.1843	0.3676	0.7651	1.8439	
96	0.0595	0.1059	0.1892	0.3794	0.7877	1.8859	
98	0.0604	0.1086	0.1950	0.3916	0.8106	1.9324	
100	0.0622	0.1123	0.2020	0.4056	0.8363	1.9791	
102	0.0653	0.1173	0.2096	0.4201	0.8623	2.0280	
104	0.0701	0.1241	0.2189	0.4363	0.8904	2.0723	
106	0.0775	0.1336	0.2313	0.4557	0.9213	2.1219	
108	0.0895	0.1478	0.2483	0.4800	0.9553	2.1751	
110	0.1104	0.1709	0.2738	0.5127	0.9991	2.2405	
112	0.1512	0.2141	0.3188	0.5644	1.0602	2.3207	
114	0.2487	0.3150	0.4192	0.6696	1.1741	2.4569	
116	0.5872	0.6636	0.7561	1.0032	1.5169	2.8235	

Table 8: Opacity-weighted mean kinetic temperature, T_k, in K corresponding to the conditions for the ranked opacities in Table 7.

Frequency (GHz)	Percentile, Ranked by Opacities						
	Best	***0.10***	***0.25***	***0.50***	***0.75***	***0.90***	***Worse***
2	270.3	268.5	269.4	261.2	253.4	265.6	244.7
3	269.5	269.6	266.9	257.2	253.1	265.0	263.0
4	269.8	268.4	265.7	270.3	258.1	262.8	262.7
5	265.5	269.5	255.8	271.3	268.5	272.7	262.8
6	265.6	269.0	271.6	269.1	250.6	266.4	263.1
7	265.8	258.0	267.0	268.2	256.2	271.5	263.5
8	265.9	259.5	248.8	265.7	275.2	271.1	264.1
9	266.0	257.2	270.4	273.3	278.0	272.3	264.8
10	266.2	263.7	255.3	272.8	272.4	272.3	265.4
11	266.4	256.8	266.5	274.6	277.9	271.9	266.0
12	259.9	253.3	264.6	262.6	278.9	272.0	266.5
13	259.7	264.6	268.5	274.2	279.3	269.7	267.0
14	259.8	249.0	271.8	277.0	267.1	269.3	282.1
15	259.9	255.1	258.9	277.7	269.9	271.2	282.3

Frequency (GHz)	Percentile, Ranked by Opacities						
	Best	***0.10***	***0.25***	***0.50***	***0.75***	***0.90***	***Worse***
16	260.0	267.6	264.6	278.6	268.2	276.6	282.5
17	260.2	258.7	260.1	283.1	280.9	280.4	269.0
18	260.3	270.2	275.5	278.7	280.1	271.8	269.7
19	260.7	257.6	273.9	283.2	285.7	276.2	270.4
20	244.9	255.8	263.1	269.2	282.3	276.3	271.3
21	244.1	254.2	264.0	284.7	284.6	279.3	272.3
22	240.7	244.1	266.2	265.3	273.6	281.0	272.0
23	245.0	256.6	274.5	265.0	281.7	274.2	273.4
24	244.7	249.2	276.9	285.0	282.3	277.2	273.4
25	245.0	255.0	265.1	271.7	284.6	279.5	273.1
26	260.9	259.1	267.0	280.8	284.2	276.1	273.0
27	260.6	261.6	265.1	274.6	281.7	284.9	273.0
28	260.3	263.6	260.4	281.4	283.6	277.0	273.1
29	260.3	261.1	273.0	283.3	283.5	277.5	273.3
30	260.2	261.0	261.3	284.3	273.8	271.7	273.5
31	260.1	267.6	252.7	266.9	280.2	277.0	273.7
32	260.0	265.2	269.6	275.4	274.3	270.8	274.0
33	260.0	260.1	260.4	267.9	270.9	273.4	274.3
34	259.9	261.6	271.9	281.4	270.7	264.2	274.5
35	259.9	260.0	271.2	279.7	264.7	274.9	274.8
36	259.9	261.4	256.9	283.6	264.6	270.8	
37	259.9	259.1	270.4	279.3	271.4	273.0	
38	259.9	265.7	269.3	275.9	267.4	272.6	
39	259.9	250.7	274.1	277.1	271.3	273.1	
40	259.9	268.2	254.0	280.2	271.2	272.5	
41	259.9	258.7	268.6	261.7	270.6	270.8	
42	260.0	258.6	268.3	279.5	270.2	270.7	
43	260.0	257.2	247.9	267.6	283.3	270.6	
44	260.1	258.5	267.0	278.3	269.9	270.7	
45	260.4	254.7	268.6	278.7	270.3	270.6	
46	260.6	247.9	272.5	270.3	278.6	273.8	
47	260.8	258.7	256.2	277.8	278.0	270.5	
48	267.5	258.1	273.3	275.1	278.0	278.3	
49	267.7	259.5	250.5	275.6	272.4	270.3	
50	268.2	250.1	255.9	264.3	267.0	277.8	
68	270.0	259.9	264.8	278.0	281.6	275.6	
70	268.6	259.9	270.9	270.4	283.7	271.5	
72	261.4	257.6	251.6	269.0	284.2	271.7	
74	261.3	262.6	262.8	272.6	278.9	262.7	
76	261.3	261.2	270.9	260.0	264.5	280.6	
78	261.4	257.5	271.8	282.7	283.3	278.7	
80	261.5	269.6	262.2	282.8	286.0	277.9	
82	261.7	260.7	264.0	285.2	287.6	274.0	
84	261.8	267.7	276.8	283.3	282.4	285.5	
86	262.0	262.9	260.0	264.5	286.6	284.5	
88	262.1	267.9	273.6	280.9	274.1	274.2	
90	262.2	264.4	277.5	269.1	285.4	274.3	
92	262.3	269.1	262.8	285.2	267.6	282.3	
94	262.3	263.2	280.3	287.0	285.8	281.1	
96	262.3	268.1	277.9	267.8	283.8	282.5	
98	262.3	265.3	273.9	280.8	286.0	282.6	
100	262.2	265.9	283.0	272.1	280.4	290.8	
102	262.0	265.2	278.7	285.6	280.4	272.7	
104	261.8	262.8	275.5	287.5	283.7	289.5	
106	261.5	266.2	270.2	286.1	273.5	286.7	
108	261.1	265.7	266.1	282.5	281.6	291.1	
110	260.6	266.6	277.9	284.4	262.3	286.8	
112	260.1	260.5	267.7	285.0	269.1	286.7	
114	259.6	266.3	263.4	269.2	267.2	277.7	
116	259.9	262.8	273.2	273.1	282.1	278.2	

Table 9: Adopted values for receiver noise temperatures.

Frequency (GHz)	***Receiver Noise Temperature (K)***	***Frequency (GHz)***	***Receiver Noise Temperature (K)***	***Frequency (GHz)***	***Receiver Noise Temperature (K)***
2	6.0	27	16.6	68	40.0
3	6.0	28	18.8	70	40.0
4	9.0	29	12.7	72	40.0
5	7.4	30	11.0	74	40.0
6	8.6	31	10.1	76	40.0
7	12.0	32	16.6	78	40.0
8	21.6	33	19.4	80	45.0
9	12.8	34	12.5	82	50.0
10	10.9	35	25.7	84	60.0
11	15.2	36	24.1	86	65.0
12	21.7	37	34.9	88	75.0
13	12.5	38	35.1	90	75.0
14	10.3	39	31.1	92	70.0
15	8.9	40	46.6	94	65.0
16	12.0	41	38.2	96	60.0
17	12.0	42	33.0	98	55.0
18	41.7	43	36.3	100	50.0
19	19.7	44	37.4	102	50.0
20	17.5	45	43.0	104	50.0
21	16.2	46	39.1	106	50.0
22	16.6	47	47.2	108	50.0
23	20.9	48	48.8	110	50.0
24	20.0	49	64.8	112	50.0
25	24.3	50	113.3	114	50.0
26	25.3			116	50.0